Mode Transition in a Low-current LaB_6 Hollow Cathode for Electric Propulsion Systems for Small Satellites

IEPC-2019-427

Presented at the 36th International Electric Propulsion Conference,
University of Vienna, Austria
September 15-20, 2019

George-Cristian Potrivitu[1], Luxiang Xu[2], Igor Levchenko[3,*], Shiyong Huang[4], Yufei Sun[5], Muhammad Wisnuh Aggriawan bin Rohaizat[6], Jian Wei Mark Lim[7,**] Kateryna Bazaka[8,***], and Shuyan Xu[9]
Plasma Sources and Application Centre/Space Propulsion Centre, NIE, Nanyang Technological University, Singapore 637616
[*] *School of Chemistry, Physics, and Mechanical Engineering, Queensland University of Technology, Brisbane, Queensland 4000, Australia.*
[**] *Energy Research Institute (ERI@N), Nanyang Technological University, Singapore 637553*
[***] *Research School of Electrical, Energy and Materials Engineering, The Australian National University, ACT 2601, Australia*

Abstract: Hollow cathodes are critical components of many space solar electric propulsion systems drastically influencing the performance and lifetime of the overall system. The PSAC LaB_6 laboratory model cathode was systematically tested with Krypton in diode and triode configuration with an external disc anode and keeper electrode while mode transitions were observed over a wide range of discharge current (0.1 to 1 A), keeper current (0 to 0.2 A) and mass flow rate (0.1 to 0.25 mg s^{-1}-Kr). The influence of the keeper current as well as the mass flow rate on mode transition was analyzed leading to a comprehensive results matrix which allows for the proper control of the cathode in the most efficient discharge mode, *i.e.* spot mode. Moreover, the thermal aspect of the model cathode was investigated, and the results were compared with thermal simulations in order to support the future improvements of the thermal management of the cathode. The results suggested the need for an improved thermal shielding and the reduction of thermal conduction from the emitter region to the cathode base to achieve lower start-up power requirements as well as auto-thermal (self-sustained) functioning.

Nomenclature

D_o	= cathode orifice diameter	TC	= thermocouple
I	= discharge current	V	= potential/voltage
j	= current density	W	= atomic mass number
J_0	= equivalent mass flow rate	ΔV	= potential drop
ID	= inner diameter	ε	= emissivity
OD	= outer diameter	ε_i	= ionization potential
PSAC	= Plasma Sources and Applications Centre	κ	= thermal conductivity
SPCS	= Space Propulsion Centre Singapore	σ	= ionization cross section

[1] PhD Candidate, PSAC/SPCS, nie17potr7281@e.ntu.edu.sg
[2] Research Engineer, PSAC/SPCS, luxiang.xu@nie.edu.sg
[3] Research Fellow, PSAC/SPCS/QUT, levchenko.igor@nie.edu.sg
[4] Research Fellow, PSAC/SPCS, shiyong.huang@nie.edu.sg
[5] PhD Candidate, PSAC/SPCS, nie17suny6686@e.ntu.edu.sg
[6] PhD Pre-candidate, PSAC/SPCS, muhammad255@e.ntu.edu.sg
[7] Research Scientist, PSAC/SPCS/ERI@N, marklimjw@ntu.edu.sg
[8] Professor, ANU, katia.bazaka@anu.edu.au
[9] Professor, PSAC/SPCS, shuyan@ntu.edu.sg

I.Introduction

THERMIONIC hollow cathodes remain instrumental for the functioning of several types of electric propulsion devices, including Hall thrusters. Although based on a rather simplistic geometry, a hollow cathode produces a partially-ionized plasma, while the gas flow spans over a wide range of conditions from Poiseuille flow, to viscous and compressible, ending with supersonic electrons drifting out of the cathode orifice[1,2]. Due to the non-equilibrium ionization nature of the hollow cathode discharges[1], the plume of such devices is characterized by the emergence of plasma turbulences and instabilities which may in turn negatively impact the performances of the entire propulsion system, for instance a Hall thruster. It is therefore important to design and manufacture hollow cathodes that can operate in a stable, self-sustained mode, while emitting the necessary current to maintain the thruster discharge and neutralize the thruster's plume.

In the latter years, the emergence of the "new space" sector is imposing new constrictions to the satellite propulsion systems, small footprint and low power consumption, driven by the miniaturization of the satellite platforms[3,4,28-30]. Hall thruster is a mature electric propulsion technology with a long space heritage. However, the miniaturization of such systems is a complex endeavor and comes with a significant loss in efficiency. Moreover, classical Hall thrusters depend on hollow cathodes which in turn may increase the power consumption of the entire system, especially during start-up. In order to minimize the power consumption of a Hall thruster system for a small satellite, catered at around 50 W of discharge power, the cathode should consume not more than 50 W for the start-up, *i.e.* heating phase, and should produce a stable discharge in a self-sustained mode. The cathode mass flow rate should be also reduced to minimum in order not to impact the propulsion system overall efficiency.

It is known that hollow cathode discharges exhibit two main operational modes: spot and plume. Spot mode operation remains the desired one because the cathode's anode and the keeper voltage are relatively low and seem stable for a fixed anode/keeper current, developing only small temporal variation. Plume mode operation is characterized by high variations in anode and keeper voltage. A significant drawback of the plume mode is the emergence of very energetic backflow ions which are repelled by the anode or the keeper electrode, accelerating them towards the cathode surface, causing high sputtering rates, thus, limiting the cathode's lifetime. In order to distinguish between the two modes, one of the options is to apply a mode criterion. Developed by Sary *et al.* and based on plasma simulations and experimental results, the discharge mode criterion makes use of the time waveforms of the anode current and states the following: spot mode corresponds to the ratio of the anode current's standard deviation to anode current's mean value, $I_{a,std}/I_{a,mean}$, being under 9%, while plume mode corresponds to ratios over 9%[5-8]. Departing from the time waveforms of the anode current recorded during the tests, the power spectral densities (PSD) can be computed. The PSDs deliver information about the frequency range of the main instabilities that may emerge in the cathode plume. Plume modes are expected to be characterized by noisy, more energetic spectra, with higher intensities and frequency peaks in the range 10-150 kHz. These are the characteristics of ionization-like instabilities[2,7-12]. Spot modes, on the other hand, have quiescent, less energetic spectra. This information, correlated with the abovementioned criterion helps in determining the cathode operating mode in a robust way, in comparison to the interpretation based on Brophy criterion which states that the plume mode is characterized by peak-to-peak anode voltage values of over 5 V[15]. It is therefore imperative to design cathodes that can operate in spot mode while delivering the required emission current. Therefore, mode transition in hollow cathodes for electric propulsion together with comprehensive discharge mode matrices bolster the understanding of such devices and the design efforts for miniaturized, efficient and low-power consuming hollow cathode.

This paper presents the results obtained using a laboratory 1 A-class LaB_6 cathode, referred hereinafter to as PSAC cathode, operated with Kr. The choice of Kr over Xe is justified due to the lower cost of the former, while at our laboratory Hall thrusters have been extensively tested using Kr or a combination of the two, thrust head on Xe and cathode on Kr[3,19,20]. The paper presents a simple approach in constructing a comprehensive test matrix for low-current hollow cathode operation based on extensive testing; cathode operation in diode configuration with the external anode, and cathode operation in triode configuration with both the external anode and the keeper electrode. The cathode discharge mode is derived for a range of anode current from 0.1 to 1 A and keeper current from 0.05 to 0.2 A. The cathode mass flow rate was also varied from 0.1 to 0.25 mg s^{-1}-Kr. Thermal management is crucial for hollow cathodes in order to achieve low start-up heating power and self-sustained operation. This becomes even more important for emission current levels less than 1 A. This paper presents the thermal characterization tests conducted for PSAC cathode and includes a discussion on further improvements of the cathode design.

II.Experimental setup

PSAC cathode[3] is based on a LaB_6 hollow emitter with ID 2 mm and OD 4 mm. Having a length of 10 mm, the emitter has a emission surface area of 0.62 cm^2. The 0.5 mm thick orifice plate is made of the same material as the insert, providing an orifice of 1 mm in diameter and an additional emission surface area of 0.13 cm^2, leading to a total emission surface area of 0.76 cm^2. Both the emitter and the orifice plate are kept in place by a graphite holder. To the graphite holder, the gas line is attached; an ID 0.5/OD 0.8 mm tantalum tube. The heater is made of two concentric boron nitride parts: one part holds the 0.3 mm-diameter and 284 mm long heating filament made of tungsten, and the second part encapsulates the former elements. To reduce the heat loss and improve the heating efficiency, thin tantalum foils are wrapped around the heater and behave as a thermal shield. The internal parts of the cathode are protected by a stainless steel keeper with a graphite keeper orifice plate. The keeper is a hollow cylinder ID 16/OD 18 mm and approximately 36 mm long, while the graphite orifice plate has a 1 mm-diameter orifice. The internal parts are fixed to the stainless steel cathode base by press fitting via the gas line tube and a Swagelok fitting. A ceramic insulator (BN-CrO) is placed between the keeper and the base. The current return for the heating filament is made via the common ground (cathode connection). A schematic depicting the main components of the cathode is shown in Fig. 1.

The cathode was designed to provide sufficient emission current, typically under 1.0 A, for the low-power Hall thrusters developed at PSAC/SPCS. In order to achieve such temperatures, the cathode heating power reaches over 65 W. Moreover, for a stable operation, the cathode requires a small keeper current. Such a large heating power is a major drawback for the entire propulsion system, since the goal is to reduce the overall power consumption of the Hall thruster to 50 W or less. Therefore, the cathode heating and ignition power should be, ideally, under 50 W.

The cathode was tested in diode and triode configuration in the Cathode Experiments Vacuum Chamber (CEVAC) at PSAC/SPCS, depicted in Fig. 2-*a)*. The chamber is made of stainless steel and has a diameter of 0.4 m with a capacity of 40 l. The pressure inside the chamber can reach 5×10^{-6} mbar-N_2 and is attained by using a KYKY RVP-6 dry rotary pump and a 600 l s^{-1} KYKY FF 160/620E turbomolecular pump to evacuate light gases. The chamber is accessed through a 0.4 m-diameter door located at the top of the chamber. The pressure is measured by ZHVAC pressure gauge controller with sensors for low vacuum (down to 10^{-3} mbar-N_2) and high vacuum (down to 10^{-6} mbar-N_2) and corrected for Kr. The cathode was operated with Kr, 99.999% purity. The gas was supplied at 1.5 bar from a pressurized tank. The gas mass flow rate is controlled with a Sevenstar D07 Series mass flow controller calibrated for Kr.

Apart from the electrical measurements that are discussed in the following Section, the chamber was equipped with several K-type thermocouples. The thermocouples output was read and recorded using BERM Rex C-100 PID controllers. Most of the thermocouples were rated for temperatures up to 673.15 K, while some of them were rated for 1648.15 K. Using this last type of thermocouples, the internal temperature in the emitter region was recorded.

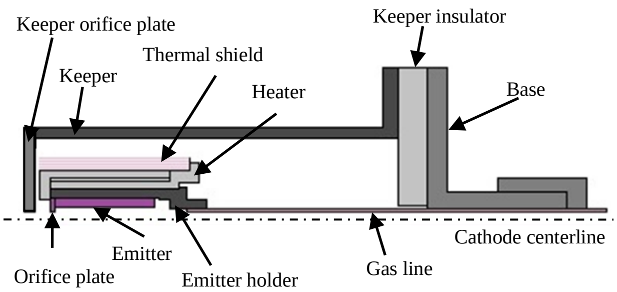

Figure 1. Schematic of PSAC LaB_6 hollow cathode.

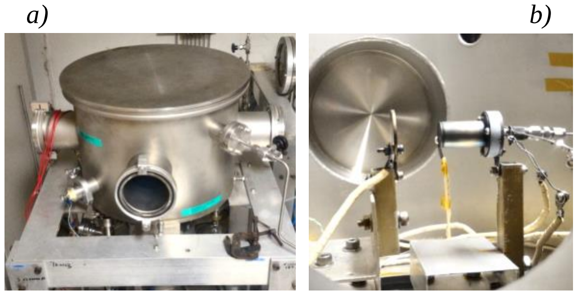

Figure 2. *a)* Cathode Experiment Vacuum Chamber (CEVAC) and *b)* PSAC cathode installed in CEVAC with the external anode (a K-type thermocouple is visible, touching the cathode's keeper electrode).

The cathode was installed in CEVAC together with an external disc anode, as depicted in Fig. 2-*b)*. The anode is a stainless steel disc with a surface area of 5.6 cm^2. The anode was placed at 25 mm downstream of the cathode exit plane. The anode surface area and the cathode-anode distance replicate the same conditions as when the cathode is operated with a Hall thruster. The discharge between the keeper and the cathode (grounded), *i.e.* the secondary discharge is provided by a HSPY-600 DC power supply (0-999.9 V, 0-0.5 A). The primary or main discharge between the cathode (ground) and the external anode is maintained by a NolePower DC power supply (WYK-100001 CK, 0-999.9 V, 0-1 A). The heating power is delivered by a Frederiksen SF 0-24 V AC/DC power supply. Anode-cathode discharge current, referred to as the anode current, I_a, was measured using a Pearson wideband current monitor (time variation, 0.025 V per A). The anode voltage, V_a, and the keeper voltage, V_k, were measured using voltage probes: Tektronix P5100 (250 MHz, 2.75 pF) and Yokogawa 700988 (400 MHz, 14 pF). The probes were connected to a Yokogawa digital oscilloscope (DLM2024, 200 MHz, 2.5 GS s^{-1}). The electrical waveforms were recorded at sampling frequency of 500 kHz, assuring a cut-off frequency of 250 kHz. This frequency is high enough to catch the usual oscillating phenomena that the anode current and voltage may exhibit in the plume of a low current cathode[7,8].

For the results presented hereinafter, the main systematic uncertainty comes from the power supplies, the current/voltage probes and the oscilloscope. For the current/voltage measurements the following uncertainty is considered: power supply accuracy (0.5%/0.1%), probe accuracy (1%/2%), oscilloscope resolution (8 bits) and accuracy (1.5%). All those account for systematic uncertainty. The random uncertainty is taken as the standard deviation of the mean of the measured current/voltage values.

For temperature measurements, uncertainty in the results is induced by the thermocouple and the controllers. The K-type thermocouples used in this study induce an uncertainty of $\pm 2.5°C$ and they have an accuracy of $\pm 0.75\%t$. BERM Rex C-100 controller has an accuracy of 0.5%, while the MAX31855 temperature sensors induce uncertainty of $\pm 2°C$.

In the following sections the results for the cathode discharge and thermal characterization are presented followed by a discussion of the main findings and future developments on low-current hollow cathodes at PSAC/SPCS.

III. Cathode discharge characterization

In order to construct the cathode operating envelope, *i.e.* discharge characteristics, the cathode was operated with Kr in diode configuration with the external anode and in triode configuration with both the external anode and the keeper electrode.

Two sets of mass flow rates were chosen: low mass flow rates (0.10 mg s^{-1}, 0.12 mg s^{-1} and 0.15 mg s^{-1}) and high mass flow rates (0.18 mg s^{-1}, 0.21 mg s^{-1} and 0.25 mg s^{-1}). The anode current was varied from 0.1 A to 1.0 A with an increment of 0.1 A up to 0.6 A, followed by an increment of 0.2 A henceforth. The keeper current was varied from 0.05 A to 0.20 A with an increment of 0.05 A. At low mass flow rates, only three values of the keeper current were tested: 0.10 A, 0.15 A and 0.20 A due to the instable operation of the cathode at lower keeper currents. Moreover, at 0.10 mg s^{-1} the cathode discharge was unable to be sustained at anode current above 0.6 A. At higher mass flow rates, the cathode was also run with no keeper current, in diode configuration with the external anode.

In order to start the cathode discharge, the heating power was gradually increased over 10 min to approximately 68 W. The cathode mass flow rate was set to 0.10 mg s^{-1} and the secondary discharge was established imposing a keeper voltage, V_k, with a keeper current, I_k, of 150 V limited at 0.10 A. Once the secondary discharge is established, the primary discharge was enabled by biasing the external anode at an anode voltage, V_a, of 200 V and limiting the anode current, I_a, to 0.10 A. All measurements were conducted with the anode and keeper power supplies operating in a "current regulated" manner. It is worth stating that all measurements were conducted with the cathode receiving a heating power of approximately 68 W, kept constant throughout the experiments. Therefore, the cathode was not operated in self-sustained mode. However, PSAC cathode was proven to operate in self-sustained mode at roughly 0.75 A of discharge current while operating with a Hall thruster at Xe mass flow rates as low as 0.02 mg s^{-1}. Between each change in the mass flow rate or anode/keeper current, the cathode was allowed to run for 300 s before any current/voltage probe measurements were recorded. This was to ensure a stable operation of the cathode at each new operating condition.

The cathode operating envelopes are presented hereinafter. The cathode operating mode (spot/plume) and mode transition were assessed based on the time waveforms of the anode current by employing the following discharge mode criterion presented in the Introduction. Two discharge mode maps are shown containing a global picture of the spot/plume mode range as a function of the cathode discharge characteristics. In order to visualize the influence of keeper electrode over the cathode discharge power as well as the anode discharge impedance and cathode overall discharge power, the results for 0.12 mg s^{-1} and 0.21 mg s^{-1} are also presented.

Table 1. Test matrix for 0.21 mg s^{-1} and the cathode operating mode for each tested point

Keeper current, A	Anode current, A							
	0.10	0.20	0.30	0.40	0.50	0.60	0.80	1.00
0.00	-	Plume	Plume	Spot	Spot	Spot	Spot	-
0.05	Plume	Plume	Plume	Spot	Spot	Spot	Spot	Spot
0.10	Plume	Plume	Plume	Spot	Spot	Spot	Spot	Spot
0.15	Plume	Plume	Plume	Plume	Spot	Spot	Spot	Spot
0.20	Plume	Plume	Plume	Plume	Spot	Spot	Spot	Spot

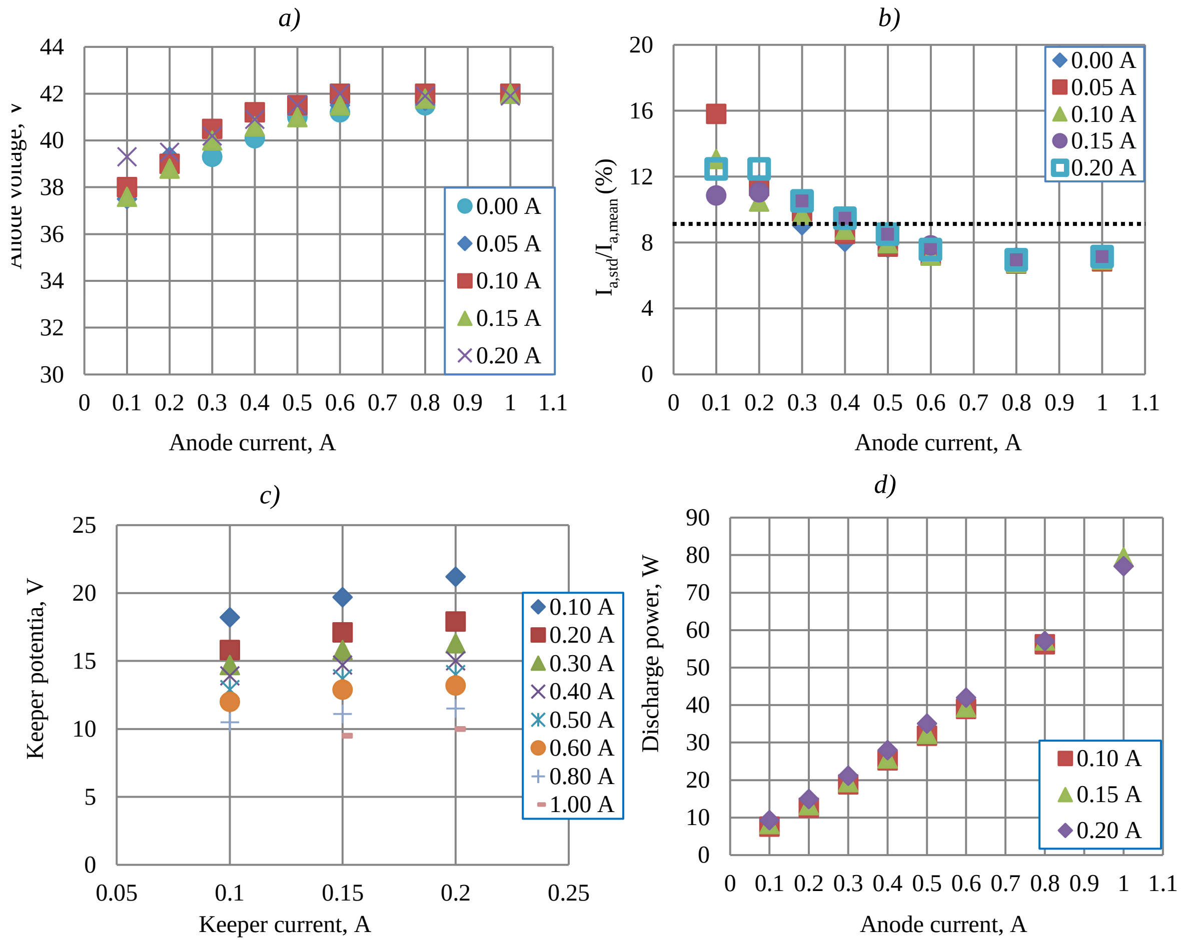

Figure 3. Cathode discharge characteristics for 0.21 mg s^{-1}-Kr: *a)* anode voltage as a function of anode current and for different keeper current values, *b)* ratio $I_{a,std}/I_{a,mean}$ as a function of anode current and for different keeper current levels (the dashed line at 9% shows the spot/plume threshold) and for 0.12 mg s^{-1}-Kr: *c)* keeper voltage as a function of keeper current and for different anode current values, and *d)* total discharge power as a function of anode current and for different keeper current values.

The test matrix for the mass flow rate of 0.21 mg s^{-1} and the corresponding cathode discharge mode observed are presented in Table 1. Such a test matrix was constructed for each mass flow rate value. The anode *I-V* characteristics are depicted in Fig. 3-*a)*. One can observe that in the case of higher mass flow rate, the keeper current has little influence on the anode discharge characteristics. The anode voltage ranges from 37 to 42 V, with an increase over the range of 0.30- 0.60 A of anode current, followed by a plateau for anode current levels higher than 0.60 A. Therefore, the positive discharge impedance is observed for discharge current under 0.6 A, followed by a relatively constant impedance. This tendency was observed for all high mass flow rates, while for low mass flow rates only positive discharge impedance was observed over the entire range of discharge current.

At this mass flow rate the cathode showed both plume and spot mode operation. The plume mode operation was recorded for anode current values below 0.30 A, while over this value the cathode discharge transitioned to spot mode operation. The fluctuations in the anode current ranged between 7 and 16% of the average value, as depicted in Fig. 3-*b)*. Moreover, the cathode exhibited a stable operation without a keeper current. Keeper *I-V* characteristics for the mass flow rate of 0.12 mg s^{-1} are presented in Fig. 3-*c)*. The increase in anode current induces a decrease in keeper voltage, while the overall discharge power remains constant at each operating point, regardless the keeper current value, see Fig. 3-*d)*. Moreover, the keeper voltage increases rapidly when the keeper current is increased, ranging from 9.5 to 21.5 V, over the entire range of tested anode current and keeper current. One of the existing theories regarding the cathode discharge modes was established by Csiky[13]. The explanation revolves around the discharge current balance which includes current density fluxes made up of thermionic electrons and thermal ions and electrons at the emitter and anode/keeper surfaces. At high mass flow rates or high anode/keeper currents, the discharge plasma has high enough densities in order to sustain a passive electron current towards the keeper electrode and the anode. Thin, electron repelling sheaths are formed near the

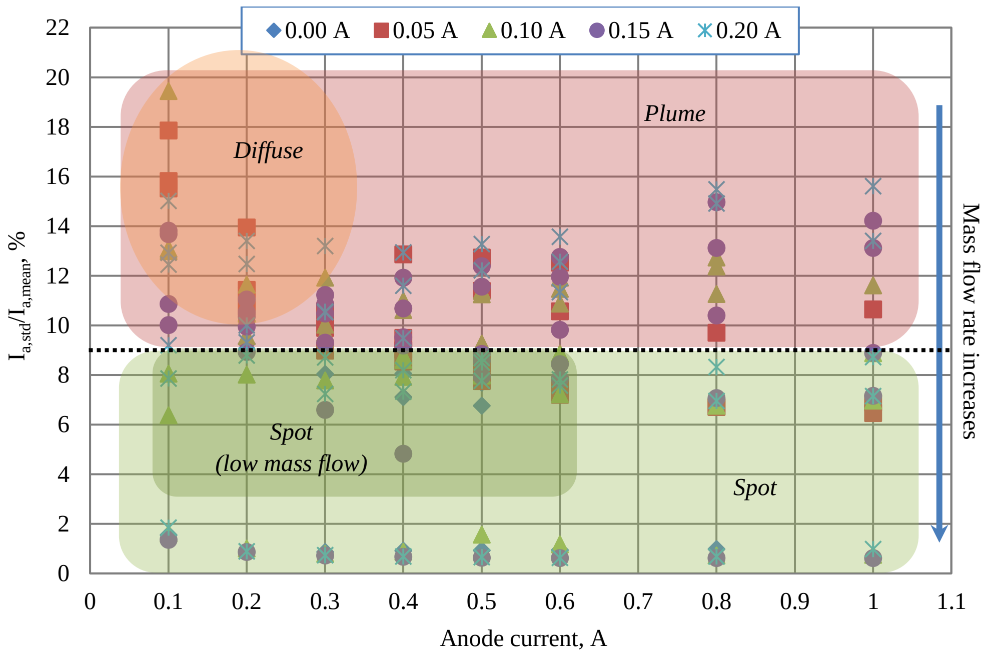

Figure 4. Cathode discharge modes for keeper current of 0 A, 0.05 A, 0.10 A, 0.15 A and 0.20 A. The dashed line at 9% shows the spot/plume threshold.

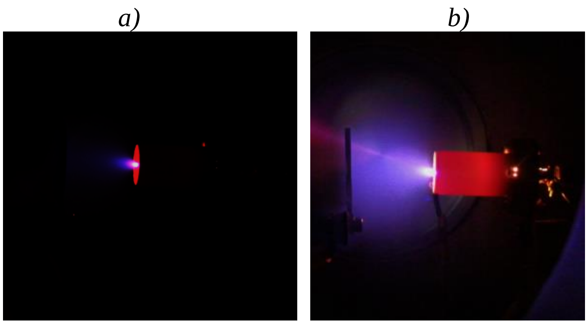

Figure 5. PSAC cathode operating in CEVAC in *a)* spot mode and *b)* plume mode.

anode and keeper surface due to a strong collisional regime characterized by low electron temperatures. Those sheaths form only when the passive plasma currents collected by the anode or the keeper are sufficient or more the net current needed for proper functioning. Usually the keeper or anode potential remains under the plasma potential during the spot mode[15]. During this operating mode the anode and the keeper potential are relatively low and seem stable for a fixed anode/keeper current, developing only small temporal variation. Visually, the cathode plume is focused close to the cathode orifice ("spot-like" bright structure), displaying a blue coloring due to the high density of Xenon ions[7,8,13]. The fast electrons produced by the cathode in this operating mode induce ionization and excitation of the neutral atoms near the cathode tip, while the rest of the cathode-anode space remains dark (less luminous)[13]. The mode is characterized by higher current densities and lower electrical resistance of the discharge[13].

On the other hand, when the passive current to the anode or the keeper are not enough to sustain the desired anode/keeper current, electron attracting sheaths form and increase the collected current towards the keeper and anode. This happens at low mass flow rates or low anode/keeper currents. The low plasma density fails to produce the necessary current while the anode and keeper voltages start to increase due to the formation of thick, electron attracting sheaths[15]. In this way the plume mode is established. Within the electron attracting sheaths high energy electrons produce the excitation and ionization of the neutrals. As the mass flow rate is reduced, the sheaths increase in size and obstruct the plasma flow out of the cathode orifice. Visually, the plume of a hollow cathode operating in plume mode is less focused with a larger divergence and very bright with colours that characterize high contents of excited neutrals instead of ions. The ionization and excitation events occur in this mode in the far field plume too and they are produced by fast electrons escaping the sheath formed in front of the orifice[13]. This sheath can be visualized as a well-defined "dark space" separating the bright region next to the cathode tip and the more diffuse region attached to the anode[7,8]. Moreover, during the plume mode large variations in the anode and keeper voltages were observed. Higher electron temperatures are noticed since the plasma density is lower, allowing for a less collisional environment[13].

During experiments, the cathode exhibited both plume and spot mode operation over the entire range of tested anode and keeper current values. Figure 4 gathers together all cathode discharge mode points according to the discharge mode criterion and for the various keeper current and the two mass flow rate ranges. The ratio

$I_{a,std}/I_{a,mean}$ varied from under 1% at high mass low rate to almost 20% at lower mass flow rates. For the case of *low mass flow rate*, the cathode discharge was characterized by spot mode operation only at anode current value under 0.6 A, while plume mode operation was recorded over the entire range of anode current values. The spot modes were characterized by a lower anode voltage compared to the plume modes. The spot modes were observed to have lower anode voltage and therefore lower impedance of the discharge with lower discharge power. Visually, the spot modes were not characterized by the widely accepted description in literature[7-9,13,16]: instead of a sole blight spot at the exit plane of the cathode, a luminous plume was observed, attached to the anode, as depicted in Fig. 5-*a)*. However, the plume is much less luminous than in the case of the plume mode operation, see Fig. 5-*b)*. The brightness of the far field plume in the plume mode is due to the energetic electrons escaping the plasma sheaths formed at the cathode exit plane, producing excitation and ionization in the anode region[7,8,13].

For the *higher mass flow rate* case, the cathode operated in spot and plume mode over the entire range of anode current, depicting in general a lower discharge impedance than in the case of low mass flow rate. The plume modes at low anode current values were characterized by both low and high anode voltage. The operating points at low anode current and low anode voltage were characterized by diffuse plumes attached to the chamber walls with high luminosity, previously reported in literature as the diffuse mode[16]. As expected, for both cases, the cathode discharge impedance was decreasing as the mass flow rate was increased.

Power spectral densities of the anode current for the same mass flow rate and keeper current, at different anode current levels are presented in Fig. 6, together with the respective time waveforms. Plume modes are characterized by “noisier” time waveforms and more energetic spectra, especially in the frequency range 10 to 150 kHz. However, for the current level of 1 A the spectrum does not present any fundamental frequency and harmonic peaks, as previously reported in literature for higher current, Xe fed cathodes[7,8].

The keeper is an important component of a cathode system with two roles: protecting the internal parts of the cathode and facilitating the initial discharge of the cathode, possibly sustaining it further. A well-designed cathode only requires a keeper current at ignition and does not require it for steady-state operation. The keeper electrode is biased positively with respect to the cathode (ground), behaving as a secondary anode. PSAC cathode ignition occurs at a keeper voltage of 150 V and current-limited to 0.10 A. Once the secondary discharge is established, the primary/main discharge is established with the external anode. The cathode discharge was unstable when running in diode configuration with the external anode, and therefore a keeper current was provided. At most of the operating points, the keeper current had no significant impact on the cathode overall discharge characteristics. The anode voltage decreases only slightly as the keeper current was increased. However, the keeper discharge power ranging 0.1 to 4.2 W was necessary to maintain the triode discharge at low mass flow rates. At higher mass flow rates, the cathode run stably in diode configuration with no keeper current.

It was also noticed that the keeper discharge power decreased as the anode discharge power increased, preserving a constant overall power over the entire range of tested anode current values, see Fig. 3-*d)*. This is an important characteristic of PSAC cathode, giving the cathode a high versatility without any increase in the discharge power. It was also observed that when run with no keeper current, at high mass flow rate, the cathode characteristics did not differ much than when run with a keeper current. A better thermal management of the cathode may be enough to eliminate the need of a keeper current during steady-state operation.

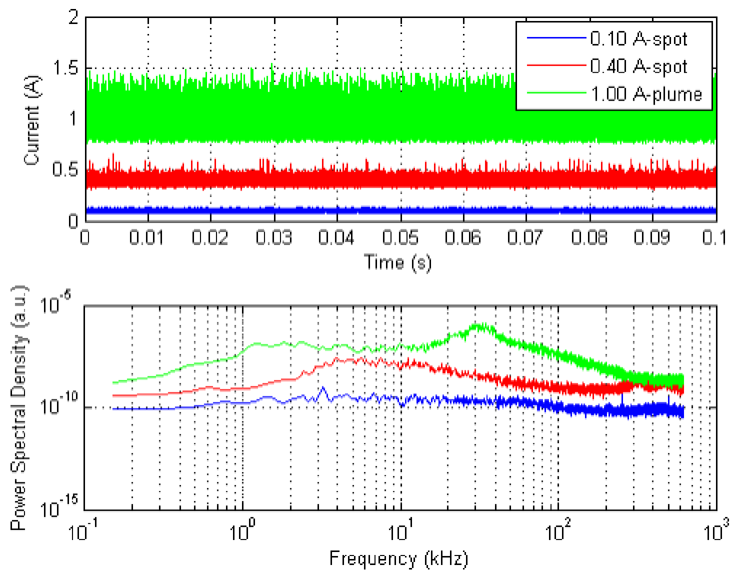

Figure 6. Time waveforms (top) and power spectral densities (bottom) of different anode current at 0.15 mg s^{-1}-Kr. The keeper current was 0.20 A.

The cathode mass flow rate has a significant influence on the cathode discharge characteristics affecting primarily the internal pressure in the emitter region and increasing the plasma density, hence reducing the plasma sheath at the emitter surface. In this way, the effective work function of the emitter is reduced via the Schottky effect[18]. As previously presented, the increase in the mass flow rate helps the cathode to transition to spot mode operation, reducing the fluctuations in the anode current due to an increase in the ionization rate. This can be clearly seen if one plots the power spectral density for a certain anode current time waveform at different mass flow rate values. As the mass flow rate is increased, the fluctuations in the time waveforms of the anode current tend to decrease and the power spectra densities magnitude decrease as well. For a mass flow rate twice the initial one, the power spectra density magnitude decreases by two orders of magnitude. This behavior of hollow cathodes was exhaustively presented in literature[7-13,16,17]. Higher cathode mass flow rate can positively influence the cathode operation and avoid the transition to plume modes, which can potentially be harmful due to the emergence of high energy ions[10]. However, when employed with a Hall thruster, the cathode mass flow rate is counted towards the overall efficiency of the propulsion system. Therefore, lower mass flow rates are ideal. A good cathode design will consider the cathode internal pressure as well as the thermal aspect, which is crucial since such devices are producing hot electrons. The thermal aspect of the cathode will be discussed in the following section.

IV. Cathode thermal characterization

Proper thermal management is instrumental for hollow cathodes with hot emitter. PSAC cathode is build based on a LaB_6 emitter heated by a metallic filament heater. In order to characterize the thermal aspect of the cathode, temperature measurements were conducted using K-type thermocouples. The experimental results are presented hereinafter. Moreover, a finite element steady-state thermal simulation was run in order to compare the simulated results with the experimental data.

A finite element model was implemented in COMSOL in a 2D axisymmetric steady-state thermal simulation (heat transfer in solids model with surface-to-surface radiation implemented). The geometry of the model is depicted in Fig. 7 as well as the various boundary conditions used to initialize the simulations. A simplified geometry was used for the simulation. For example, the heating filament was replaced by a tube with the wall thickness equal to the diameter of the heating filament diameter.

In order to refine the thermal simulation, contact thermal resistance was added between the cathode's various parts. When run at 68 W of heating power (the value required for cathode start-up during the experiments and the power continuously supplied to maintain the discharge) the thermal simulation revealed that the temperature at the emitter reaches almost 1400°C (1673.15 K), enough for a proper start-up and operation of the cathode. The cathode base temperature was used as a boundary condition in the simulation and was found out from the experiments.

The temperature measurements were conducted with the cathode heater on and in the absence of a plasma discharge or gas flow. Four K-type thermocouples (TC) were placed at various locations on the cathode, as presented in Fig. 7: TC1(a) was touching the cathode base plate, TC1(b) was inserted in the keeper insulator, through the cathode base, TC2 was placed on the outer rim of the keeper orifice plate, while TC3 was inserted through the keeper orifice and emitter orifice and reached the base of the emitter, approximately 14 mm inside the cathode. During the experiments, the background pressure in CEVAC was of 7×10^{-5} mbar.

The previous results showed that the cathode overall discharge power ranges from 5 to 80 W and remains over 60 W only for anode current values over 0.80 A. However, much of the discharge power dissipates in the cathode plume and does not participate actively in heating the emitter for a certain level of emission current. Therefore, thermal management for PSAC cathode must be improved in order to assure self-sustained operation without external heating power during the steady state operation.

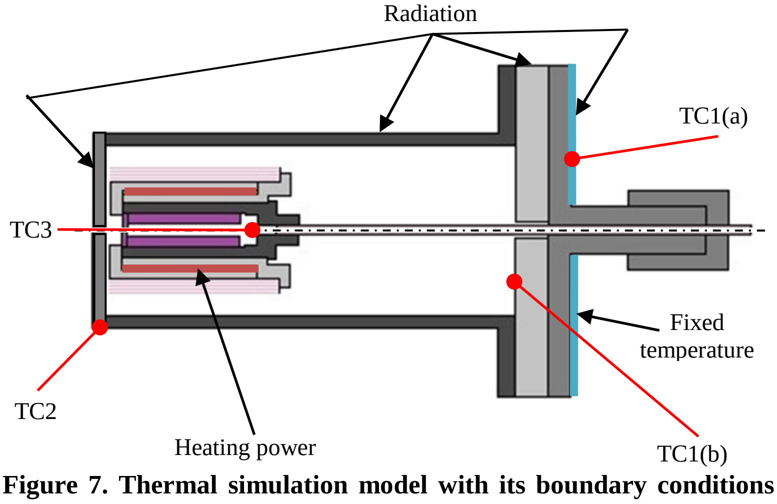

Figure 7. Thermal simulation model with its boundary conditions and the locations of the thermocouples for PSAC cathode.

The results of the measurements when 68 W of heating power is delivered to the cathode heater are presented in Table 2 and compared to the simulated results for each thermocouple location. The most important result is collected by TC3, inserted in the emitter region. For TC3, the simulation result is 139°C higher than the experimental one. Thermocouple TC3 measured a temperature of 1258°C, proving that at this temperature the cathode can provide 0.27 A of emitted current, for an emission surface of 0.76 cm^2. Nevertheless, the cathode discharge was always established at 0.10 A.

Table 2. Experimental and simulation results for PSAC cathode thermal characterization at 68 W of heating power.

Heating power		68 W			
Thermocouple		TC1(a)	TC1(b)	TC2	TC3
Temperature, °C	Experiment	240	357	525	1258
	Simulation	(imposed boundary)	450	753	1397

Thermocouple TC2 recorded the temperature at the edge of the keeper orifice plate. The temperature in this region can reach up to 525°C, due to direct power deposition from the cathode internal plasma in the keeper orifice. The experimental data is 228°C lower than the simulated one. The finite-element ideal design of the cathode includes a thermal shield that is perfectly concentric and with a specific number of foils. In reality, the thermal shield may have a lower number of winding and the distance between them can differ. Moreover, in the simulation design, the graphite keeper orifice plate is perfectly in contact with the stainless steel keeper tube, while in reality this plate is imperfectly press-fit to the tube. This can explain the differences in temperature between the simulated and experimental results.

Thermocouple TC1(a) recorded the temperature of the stainless steel cathode base. At 68 W, the base can reach up to 240°C. The temperature recorded by TC1(a) was used as boundary condition (fixed temperature) for the thermal simulation. Thermocouple TC1(b), located inside the keeper insulator recorded a temperature 117°C higher than the one recorded by TC1(a), although separated by only 6 mm of ceramic material. Since TC1(b) is exposed to the interior of the cathode, higher temperatures in this region, reaching almost 360°C, indicate significant thermal loss from the emitter region to the cathode base through conduction and radiation inside the cathode.

The temperature results give an insight on the thermal management of PSAC cathode. The rapid cooling of the cathode, once the heating power is reduced or turned off, suggests that the thermal shielding is not efficient. The high temperatures recorded at the cathode base suggest that important thermal loss due to conduction and radiation from the emitter region to the extremities of the cathode reduces the thermal efficiency of the system. Moreover, if the cathode is used for emission currents under 1 A, the emitter can be redesigned with a shorter length, smaller internal diameter and thinner walls.

V.Discussion and future developments

Understanding hollow cathode operation in standalone mode is instrumental for device optimization and prediction of cathode behavior when it is operated with a Hall thruster. Discharge mode characterization and mode transition provide valuable information on cathode discharge stability and allows for the identification of discharge current (anode and keeper) and mass flow rate range that correspond to the spot mode. PSAC cathode was systematically tested in standalone mode in diode and triode configuration with an external anode and keeper electrode in order to construct the cathode's discharge mode maps and assess for its thermal management characteristics. Although Kr is known to have a lower atomic mass and a higher ionization potential compared to Xenon, and also considering that the performance of a Hall thruster drops when this gas is used as propellant, its much lower cost and decent performance when used for hollow cathodes make it a viable choice for plasma propulsion systems for small satellite. At PSAC labs Kr was used with Hall thrusters[19,20], for both the thrust head and the hollow cathode, while other tests were conducted with the thrust head operating on Xe while the cathode was operated on Kr, with good performance[3]. Moreover, Xe-Kr mix proved to be viable for Hall thruster operation[24-27]. Therefore, testing our cathodes with Kr is important in order to establish their operation range and collect information needed for design optimization.

PSAC cathode was developed at PSAC/SPCS to run in conjunction with Hall thrusters at discharge powers ranging from 200 to 300 W. Therefore, the LaB_6 emitter was designed to sustain an emission current close to 1 A. The cathode start-up requires around 68 W of heating power and maintains self-sustained operation at very low propellant mass flow rates (0.03 mg s^{-1}-Kr) while producing 0.75 A of current for a Hall thruster[3]. However, the cathode was never tested in standalone mode.

It was observed that the keeper characteristics and total power distribution followed the same trends for all mass flow rates, while the main discharge characteristics, *i.e.* anode discharge, presented positive impedance especially at low mass flow rates and discharge current under 0.6 A. The anode potential is a sum of different potential levels within the cathode, each one being a function of the anode current and the mass flow rate (through plasma parameters such as electron density and electron temperature)[21]:

$$V_a(\dot{m}, I_a) = V_p(\dot{m}, I_a) + \Delta V_{ds1}(\dot{m}, I_a) + V_o(\dot{m}, I_a) + \Delta V_{ds2}(\dot{m}, I_a), \quad (1)$$

where V_p is the plasma potential, ΔV_{ds1} is the planar double sheath potential drop at the emitter location, V_o is the ohmic voltage drop in the orifice channel and ΔV_{ds2} is the voltage drop due to the formation of a spherical double sheath at the keeper orifice location. All the components in Eq. (1) are complex functions of plasma properties in the emitter, emitter-keeper and keeper orifice regions highly influenced by the imposed discharge current, internal pressure (function of mass flow rate) and cathode geometry. Moreover, at the emitter surface, plasma-wall interactions can be described using a first-order approximation, by balancing the current and power in the following equation[22]:

$$j_i\left(\Phi_{sh}+\varepsilon_i+\frac{2k_BT_e}{e}\right)=j\left(\Phi_{wf,eff}+\frac{2k_BT_e}{e}\right)+j_{em}\left(\frac{3}{2}\frac{k_BT}{e}-\frac{2k_BT_e}{e}\right)+\varepsilon\sigma_{SB}T^4+\kappa\frac{T-T_b}{L_c}, \quad (2)$$

where j_i is the ion current density collected at the emitter surface, Φ_{sh} is the sheath voltage at the emitter surface, ε_i is the first ionization potential of the propellant atoms, $\Phi_{wf,eff}$ is the effective work function of the emitter material, j is the total current density, while the last two terms in the right-hand side of the equation account for radiation and conduction losses, with T denoting the emitter temperature, T_b the cathode base temperature and L_c the cathode tube length. Therefore, the positive impedance characteristics at low mass flow rates and low discharge current can be explained by higher voltage drops in the double sheath regions and a possible increase in the emitter sheath potential.

During the experiments, the cathode exhibited both spot mode and plume mode operation, including a particular type of plume mode known as the diffuse mode. It was shown that spot mode appears at higher mass flow rates and discharge currents under 0.6 A, while the mass flow rate remains in the relatively low region. At higher mass flow rates, spot mode operation is observed over the entire range of discharge current. In the late '70s Rehn and Kaufman[23] provided an empirical criterion for the collision parameter to describe spot mode operation based on the equivalent mass flow rate, J_0, in amperes, and the cathode orifice diameter for different inert gases (Ar, Kr, Xe):

$$\frac{J_0\sigma\sqrt{W}}{D_o}\geq 13.9\times10^{-20}\ \mathrm{A\ m^2amu^{0.5}\ mm^{-1}}, \quad (3)$$

where σ is the maximum value of the ionization cross section of neutrals by electrons and W is the gas atomic mass number. They reported that no plume mode operation was recorded above this value and no spot operation was recorded for values under $12\times10^{-20}\ \mathrm{A\ m^2amu^{0.5}\ mm^{-1}}$. In the current work, PSAC cathode has a 1 mm-diameter orifice while the equivalent mass flow rates at which spot mode operation was recorded were 0.07 A and 0.18 A. Therefore, spot mode operation was recorded for collision parameter values down to $3.3\times10^{-20}\ \mathrm{A\ m^2amu^{0.5}\ mm^{-1}}$, at much lower discharge potentials, with biased keeper electrode and heating power on. The results revealed the impact of additional heating power during the cathode operation (since all tests were performed with the cathode receiving 68 W of heating power regardless the mass flow rate and discharge current). It is worth investigating how the expression of the collision parameter can be changed to characterize cathode operation in conjunction with a Hall thruster or when the cathode is receiving additional heating power. Additional heating power can sustain spot mode operation at low mass flow rates by supplementing the emitted electron current density, compared to the self-sustained mode. It was shown that by increasing the mass flow rate, the anode current PSDs become less energetic. Although the anode current PSDs for the plume mode operation are more energetic than the ones for sport mode, thy did not present any fundamental frequency and harmonics peaks in the range 10 to 150 kHz (see Fig. 6) as expected and previously reported in literature[7,8]. Nevertheless, the existing data about hollow cathode discharge current PSDs for operation in plume mode refer to higher current operation, over 1 A with Xe.

The thermal characterization of PSAC cathode showed that the device is not fully optimized. Operating at 68 W, the emitter region reached temperatures that are sufficient for 0.27 A of current, almost thrice the imposed current at ignition (0.1 A), while the cathode base temperature reaches high levels, suggesting that thermal loss through conduction and radiation inside the cathode make the device inefficient. Therefore, the cathode requires a constant heating temperature in order to operate, while self-sustained operation was not recorded. The results of the thermal simulation were in good agreement with the experimental data with differences remain under 150°C. E.g. the emitter region. In order to improve the thermal management of the cathode, additional thermal shields can be used, while the emitter size and cathode overall dimensions can be reduced, minimizing thermal conduction and internal radiation losses from the emitter region. Moreover, lower heating power consumption during ignition can be achieved if a stronger electric field is established between the emitter and the keeper electrode (at higher keeper voltage). This can be achieved by employing emitters presenting sharp edges. Future low-current hollow cathodes developed at PSAC/SPCS will contain such emitters.

VI.Concluding remarks

PSAC cathode was for the first time tested in standalone mode in CEVAC using krypton gas in order to construct a comprehensive discharge mode matrix. The operating envelope was constructed for eight anode current values between 0.10 and 1 A, several keeper current values between 0 and 0.2 A and for five mass flow rates ranging from 0.10 to 0.25 mg s^{-1}. The anode and keeper *I-V* characteristics helped in determining the behavior of the cathode under various conditions. By applying the discharge mode criterion, maps of the cathode discharge modes were constructed showing that at low mass flow rates, the cathode operates in spot mode at low anode current (less than 0.60 A), while at higher mass flow rates the cathode operates mainly in spot mode. Power spectra density plots of the anode current time waveforms were analyzed. The spectra did not show any fundamental frequency and harmonics peaks, as in the case of high-current Xe feed cathodes[7,8]. However, the spectra for the plume mode had larger magnitudes than that for the spot mode in the range 10-150 kHz, suggesting the emergence of ionization-like instabilities in the cathode plume.

The thermal management of a cathode is of high importance. Therefore, several thermocouples were installed at various locations on the cathode. The temperature measurements were collected and then compared to simulated measurements from a finite-element model. In general, the simulation results were higher than the experimental data, due to the simplistic model employed in the simulation. However, the difference remained under 150°C for the emitter region. During the operating envelope experiments, the cathode was receiving a fixed heating power of around 68 W. This proves that the current design cannot run in a self-sustained mode for low currents and mass flow rates of Kr. Moreover, for low mass flow rates the cathode discharge extinguished if no keeper current is applied.

Low-power Hall thrusters, operating at power levels around 50 W require hollow cathodes capable of emitting less than 0.5 A of current in self-sustained mode and ignite at heating power levels less than 50 W. If LaB_6 is used for the emitter material, the thermal management, geometry and material selection of the cathode are important[31]. Smaller cathode dimensions, additional thermal shields and the isolation of the cathode emitter/heater system using only thin and long parts, can improve the thermal characteristics of the device. Kr or Xe-Kr mix can replace Xe operation with relatively good performance, while a continuous trajectory of spot mode operation can be achieved over a relatively large range of discharge current and mass flow rate.

Acknowledgments

This work was supported by OSTIn-SRP/EDB through the National Research Foundation, and in part by the Ministry of Education Singapore through MOE AcRF (RP6/16XS). George-Cristian Potrivitu acknowledges the support from the National Institute of Education Singapore through the NIE Ph.D. Scholarship. Sun Yufei and Muhammad Wisnuh Aggriawan bin Rohaizat acknowledge the support from Nanyang Technological University Singapore through the NTU Ph.D. Scholarship. Igor Levchenko acknowledges the support from the School of Chemistry, Physics and Mechanical Engineering, Science and Engineering Faculty, Queensland University of Technology.

References

[1]Polk J. *et al.*, "Temperature distributions in hollow cathode emitters", 40th AIAA/ASME/SAE/ASEE Joint Propulsion Conference and Exhibit, AIAA-2004-4116, 2004

[2]Lev D.R., Mikellides I.G., Pedrini D., Goebel D.M., Jorns B., and McDonald M., Rev. Mod. Plasma Phys. 3, 6 (2019)

[3]Levchenko I., *et al*., Appl. Phys. Rev. 5 (2018), 011104

[4]Lev D.R. *et al.*, "The technological and commercial expansion of electric propulsion in the past 24 years", IEPC-2017-242, 35th International Electric Propulsion Conference, Atlanta, USA, October 8-12, 2017

[5]Sary G., "Modélisation d'une cathode creuse pour propulseur à plasma", Ph.D. disertation, University Paul Sabatier Toulouse III, France, September 2016

[6]Sary G. *et al.*, "Hollow cathode modelling: a first approach on scaling laws", IEPC-2015-14/ISTS-2015-b-90616, Joint Conference of 30th International Symposium on Space Technology and Science and 34th International Electric Propulsion Conference and 6th Nano-satellite Symposium, Hyogo-Kobe, Japan, July 4-10, 2015

[7]Potrivitu G.C., Joussot R. and Mazouffre S., Vacuum 151 (2018), 122-132

[8]Joussot R., Grimaud L. and Mazouffre S., Vacuum 146 (2017) 52-62

[9]Nishiyama K., Shimizu Y., Funaki I., Kuninaka H. and Toki K., J. Propul. Power 23 (2007) 513-521

[10]Mikellides I.G., Katz I., Goebel D.M., and Jameson K.K., J. Appl. Phys. 101 (2007) 063301

[11]Jorns B.A., Mikellides I.G. and Goebel D.M., Phys. Rev. 90 (2014) 063106

[12]Jorns B.A., Dodson C., Goebel D.M., and Wirz R., Phys. Rev. 96 (2017) 023208

[13]Csiky G. A., "Measurements of some properties of a discharge from a hollow cathode", NASA Technical Node, NASA TN D-4966, February 1969

[14]Brophy J.R. *et al.*, "The DS1 Hyper-Extended Mission", AIAA-2002-3673, 38th Joint Propulsion Conference, 2002

[15]Courtney D., "Development and Characterization of a Diverging Cusped Field Thruster and a Lanthanum Hexaboride Hollow Cathode", Master thesis, MIT, 2008

[16]Sakai S. *et al.*, "Discharge modes and characteristics of hollow Cathode", IEPC-2007-215, 30th International Electric Propulsion Conference, Florence, Italy, September 2007

[17]Kaufman H.R., "Technology of Electron-bombardment Ion Thrusters", Vol. 36, Advances in Electronics and Electron Physics, Academic Press, New-York, 1974, pp. 265-373

[18]Ning *et al.*, Plasma Sources Sci. Technol. 11, 2 (2009)
[19]Lim J.W.M. *et al.*, Plasma Sources Sci. Technol. 28, 6 (2019)
[20]Lim J.W.M. *et al.*, Journal of Visualized Experiments 144, e58466 (2019)
[21]Capacci M. *et al.*, *"Simple Numerical Model Describing Discharge Parameters in Orificed Hollow Cathode Devices",* AIAA-97-2791, 33rd AIAA/ASME/SAE/ASEE Joint Propulsion Conference and Exhibit, Seattle, WA, 1997
[22]Albertoni R. *et al.,* "Preliminary Characterization of a LaB6 Hollow Cathode for Low-Power Hall Effect Thrusters", IEPC-2013-137, 33rd International Electric Propulsion Conference, The George Washington University, October 6-10, Washington, D.C., USA, 2013
[23]Rehn L. and Kaufman H.R., "Correlation of Inert Gas Hollow Cathode Performance", AIAA 78-707, 13th International Electric Propulsion Conference, San Diego, CA, April 1978
[24]Nakles M.R., Hargus W.A., Delgado J.J., and Corey R.L., "A Performance Comparison of Xenon and Krypton Propellant on an SPT-100 Hall Thruster", IEPC-2011-003, 32nd International Electric Propulsion Conference, Weisbaden, Germany September 11-15, 2011
[25]Saevets P.A., Kim V.P., Grdlichko D.P., and Smirnov P.G., Procedia Engineering 185 (2017), 85-90
[26]Szabo J., Tedrake R., Kolencik G., and Pote B., "Measurements of a Krypton Fed 1.5 kW Hall Effect Thruster with a Centrally Located Cathode", IEPC-2017-26, 35th International Electric Propulsion Conference, Georgia Institute of Technology, Atlanta, GA, USA October 8-12, 2017
[27]Linnell J.A., "An Evaluation of Krypton Propellant in Hall Thrusters", Ph.D. dissertation, The University of Michigan, 2007
[28]Levchenko I., Keidar M., Cantrell J., Wu Y. -L., Kuninaka H., Bazaka K., and Xu S., Nature 562, 185 (2018)
[29]Levchenko I., Xu S., Mazouffre S., Keidar M., Bazaka K, Global Challenges 2, 1800062 (2018)
[30]Levchenko I., Bazaka K., Mazouffre S., and Xu S., Nature Photonics 12, 649–657 (2018)
[31]Levchenko I., Bazaka K., Belmonte T., Keidar M., Xu S., Adv. Mater. 30, 1802201 (2018)